Angular distribution of the longitudinal $\vec{p}\vec{p}$ spin correlation parameter A_{zz} at 197.4 MeV

B. Lorentz,* W. Haeberli, F. Rathmann,† and T. Wise
Department of Physics, University of Wisconsin-Madison, Madison, Wisconsin 53706

J. Doskow, M. Dzemidzic,‡ H. O. Meyer, R. E. Pollock, B. von Przewoski, T. Rinckel, and F. Sperisen
Department of Physics and Cyclotron Facility, Indiana University, Bloomington, Indiana 47405

P. V. Pancella
Western Michigan University, Kalamazoo, Michigan 49008
(Received 1 December 1999; published 6 April 2000)

A polarized proton beam with a large longitudinal polarization component of 0.545 ± 0.005 (96% of the total polarization) was prepared in a storage ring (IUCF–Cooler). This was achieved by means of spin precession solenoids in two of the six straight sections of the ring. A polarized hydrogen storage cell target internal to the ring was used to measure the longitudinal spin correlation coefficient A_{zz} in pp elastic scattering over the laboratory angular range 5.5°–43.5° ($\theta_{\mathrm{c.m.}} = 11.5°$–90°) with statistical errors of typically 0.025. The absolute normalization was determined to an accuracy of 2.0% by use of the identity $A_{yy} - A_{xx} - A_{zz} \equiv 1$ at $\theta_{\mathrm{c.m.}} = 90°$. The identity also allows a reduction of the scale factor uncertainty of the previously published analyzing powers and spin correlation coefficients. The results are compared to recent pp partial wave analyses and NN potential models.

PACS number(s): 24.70.+s, 13.88.+e, 13.75.Cs, 25.40.Cm

I. INTRODUCTION

In recent papers we reported measurements of analyzing power A_y and spin correlation parameters A_{xx}, A_{yy}, and A_{xz} in pp elastic scattering at eight energies between 197.4 and 448.9 MeV [1,2]. The remaining independent spin correlation parameter A_{zz} can only be measured with both beam and target polarized in the beam direction (longitudinal). Here, we report on the development of longitudinal beam polarization in the proton storage ring (''Cooler'') at the Indiana University Cyclotron Facility. This polarized 197.4 MeV beam was used in conjunction with a polarized hydrogen storage cell target [3] to measure the spin correlation parameter A_{zz} in pp elastic scattering as a function of laboratory scattering angles between 5.5° and 43.5°. Two spin precession solenoids were introduced into the storage ring to prepare longitudinal beam polarization at the location of the polarized hydrogen target.

The experimental apparatus and methods, including analysis and study of systematic effects, are very similar to those described in Ref. [1], and thus will not be discussed in detail. Measurements of pp elastic scattering were taken with vertical, horizontal, and longitudinal target polarization. The measurements with longitudinal target polarization allow determination of the product $P_z Q_z A_{zz}$ of longitudinal beam polarization P_z, longitudinal target polarization Q_z, and spin correlation parameter A_{zz}.

The measurements with horizontal and vertical target polarization are used to determine the product of longitudinal beam polarization P_z and transverse target polarizations Q_x and Q_y. This makes use of the spin correlation parameter $A_{xz} = A_{zx}$, which is known from our previous measurement at the same beam energy [1]. Under the assumption that the target polarization for the three different holding field orientations is the same, this determines the product $P_z Q_z$ which is needed to extract the angular distribution of the spin correlation parameter A_{zz}.

The absolute normalization of our previous spin correlation data, as well as the normalization of the present A_{zz} measurement ultimately depend on a measurement of the analyzing power A_y in pp scattering at 183.1 MeV [4]. An interesting check of the absolute normalization is offered by the model independent relationship $A_{yy} - A_{xx} - A_{zz} \equiv 1$ [5] at $\theta_{\mathrm{c.m.}} = 90°$. Here this relation is exploited to check the correctness of the previous calibration and to improve its absolute normalization accuracy.

The preparation of longitudinal beam polarization will be discussed in Sec. II. Section III contains an overview of the experimental apparatus. The extraction of the spin correlation parameter A_{zz} from the measured yields is discussed in Sec. IV. Section V presents the final absolute calibration of the pp spin correlation parameter. A short discussion of corrections and systematic effects is given in Sec. VI. The results for the angular distribution of A_{zz} and a comparison to theoretical predictions is given in Sec. VII. This is followed by the conclusion in Sec. VIII.

II. LONGITUDINAL BEAM POLARIZATION

A. Polarization of a stored proton beam

The polarization of an ensemble of particles with spin 1/2 is described by a vector $\vec{P}$, which is parallel to the sum $\vec{\mu}$ of

*Present address: Forschungszentrum Jülich GmbH, IKP, D-52425 Jülich, Germany.

†Present address: Physikalisches Institut der Universität Erlangen-Nürnberg, D-91058 Erlangen, Germany; working at Forschungszentrum Jülich GmbH, D-52425 Jülich, Germany.

‡Present address: Department of Radiology, Indiana University School of Medicine, Indianapolis, IN 46202.

 ©2000 The American Physical Society

the magnetic moments of all particles in the ensemble. Spin-1/2 beam polarization in a storage ring is thus fully determined by the polarization of the injected beam and the motion of the magnetic moments of the stored particles.

As a proton progresses along the closed orbit, its magnetic moment precesses around the prevailing magnetic field direction. The general, relativistic equation of the motion of the direction of a magnetic dipole travelling through electromagnetic fields is known as the BMT equation [6]. From this equation we can derive the action of the two basic field elements which we need for the present purpose:

The first element we need to understand is the vertical (y) field of a bending magnet which deflects the beam in the horizontal (x-z) plane by an angle θ, while it precesses the magnetic moment of beam particles (in their rest frame) around the y axis by an angle $\xi_B(\theta)$, where

$$\xi_B(\theta) = (g-1)\,\theta\gamma = 1.792\ 847\ 39(6)\,\theta\gamma. \qquad (2.1)$$

Here, γ is the usual relativistic kinematic parameter, and g is the g factor of the proton.

The second field element is a solenoid with an integrated field $B = \int B_z dz$ along the beam direction which precesses the magnetic moment around the longitudinal (z) direction by an angle $\xi_S(B)$, where

$$\xi_S(B) = \frac{cgB}{m\beta\gamma} = 0.89235\frac{B}{\beta\gamma}. \qquad (2.2)$$

Here, c is the speed of light in m/s, m the proton mass in eV/c^2, β the usual relativistic kinematic parameter, and B the longitudinal field integral in Tesla meters (Tm).

We now study a particle which completes a single turn around the ring, starting and ending at a point s^* somewhere on the stored orbit. As a consequence of the precession of the magnetic moment by the magnetic elements in the ring lattice, there will be a ''one-turn'' net rotation $R(s^*)$ between the initial and final direction of the moment. This rotation can be calculated easily by concatenating the individual rotations around the vertical $\{R_y[\xi_B(\theta)]\}$ and longitudinal $\{R_z[\xi_S(B)]\}$ directions due to bends and solenoids, starting at s^* and proceeding against the beam direction [see Eq. (2.3)]. These rotations may be described by 3×3 matrices, but in practice it is more elegant and more convenient to adapt the spinor formalism from quantum mechanics in which rotations are expressed as complex 2×2 matrices [7].

The one-turn rotation $R(s^*)$ is characterized by a rotation axis $\vec{n}(s^*)$, and a rotation angle Ψ which is independent of the choice of s^*. The unit vector $\vec{n}(s^*)$ which is given by the eigenvector of $R(s^*)$ is called the ''spin closed orbit,'' and $\Psi/2\pi$ is known as the ''spin tune.'' It is obvious that the component of $\vec{\mu}$ (and thus the polarization vector $\vec{P}$) which is parallel to $\vec{n}(s^*)$ is preserved. The component perpendicular to $\vec{n}(s^*)$ precesses around it and over many orbits averages to zero. Thus, the direction of the beam polarization is given by the spin closed orbit.

Normally, in a storage ring the spin closed orbit is vertical for all s^*, since the effect from transverse focusing fields averages to zero. To carry out an experiment with longitudinal beam polarization one has to provide spin rotators in the ring lattice that cause the spin closed orbit at the target $\vec{n}(s_{\text{target}})$ to point along the beam direction. For energies below a few GeV, it is best to use solenoid fields to rotate the spin. In the next section we describe how this was done in the IUCF Cooler.

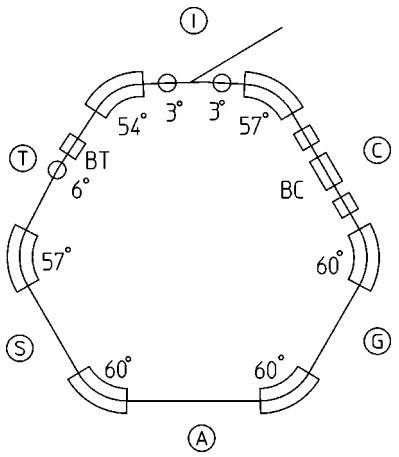

FIG. 1. The magnet lattice of the IUCF Cooler. The target is located in the *A* region. Bending magnets are marked with the bending angle in degrees. The spin precession solenoids in the *T* and *C* region are shown to illustrate their position with respect to the bending magnets.

B. Preparation of longitudinal beam polarization

The IUCF Cooler storage ring is a six-sided synchrotron with a polarized hydrogen target in the *A* region straight section, as shown in Fig. 1. This figure also shows the two spin-rotation solenoids in the *C* and *T* region which were used to prepare longitudinal polarization at the target. The placement and strength of the solenoid fields is governed by the task of achieving the desired spin closed orbit, but in practice is also constrained by space requirements and by the fact that solenoids also focus the beam and thus have an impact on the ring optics.

The C-region solenoid. The electron beam which is used for phase space cooling is transversely confined by a solenoidal field. In normal operation, the effect of this field on the spin closed orbit is compensated by two additional solenoids with opposite field, immediately upstream and downstream of the cooling region. For the present experiment we operate these compensating solenoids with reversed current such that the field direction is the same for all three solenoids. In this mode, a longitudinal field integral of $B_C = 0.877$ Tm is achieved, limited by the maximum allowed power dissipation in the solenoids.

The T-region solenoid. A superconducting solenoid was placed in the *T* region (see Fig. 1). The coil of this solenoid has an inner diameter of 17.5 cm and a length of 30 cm. The insertion length of the device is 58 cm with a clear bore of 10.8 cm. The field integral of this magnet is 1.10 Tm.

With these elements present in the ring, one obtains for the one-turn rotation starting at the target

$$R(s_{\text{target}}) = R_y[\xi_B(123°)]R_z[\xi_S(B_T)]R_y[\xi_B(117°)] \times R_z[\xi_S(B_C)]R_y[\xi_B(120°)], \quad (2.3)$$

where the deflection angles 123°, 117°, and 120° are the net deflections between *A*, *T*, and *C* regions (see Fig. 1). Evaluating the eigenvector of this matrix, normalized to 1, yields the spin closed orbit at the target $\vec{n}(s_{\text{target}}) = (0.250, 0.125, 0.960)$, where the three numbers denote horizontal (x), vertical (y), and longitudinal (z) components. The fact that the polarization is not purely longitudinal is caused by the limit on the thermal load of the *C* solenoids. The field integral required for longitudinal beam polarization at the target is roughly 1.1 Tm in each solenoid. As will be discussed in Sec. IV, the angle of 16.3° of the polarization direction with the beam direction is taken into account in the analysis of the data. Aside from a small reduction in statistical accuracy (compared to pure longitudinal polarization), the measurement of the spin correlation parameter A_{zz} is not affected.

The spin closed orbit at the injection point can be evaluated analogously. The one-turn rotation in this case is given by

$$R(s_{\text{injection}}) = R_y[\xi_B(60°)]R_z[\xi_S(B_C)]R_y[\xi_B(243°)] \times R_z[\xi_S(B_T)]R_y[\xi_B(57°)]. \quad (2.4)$$

The corresponding spin closed orbit follows as $\vec{n}(s_{\text{injection}}) = (0.252, 0.953, 0.157)$. Its direction is almost vertical. Injection of vertically polarized beam loses about 5% of the injected polarization, but eliminates the technical complication of having to make use of precession solenoids in the beam line from the cyclotron to the Cooler.

III. EXPERIMENTAL ARRANGEMENT AND EVENT IDENTIFICATION

The experiment was carried out in the IUCF Cooler storage ring at the Indiana University Cyclotron Facility. The polarized target is located in the *A* region of the ring, which has low dispersion and small β function and thus is best suited for internal storage cell targets. Polarized hydrogen atoms for the target are produced by an atomic beam source. The polarized atomic beam is injected into a *T*-shaped, thin walled storage cell, located on the axis of the storage ring. The orientation of the target polarization is defined by three sets of guide field coils, and can be changed in less than 10 ms between the longitudinal (z), vertical (y), and horizontal (x) direction.

Figure 2 shows a three-dimensional representation of the detector setup used to detect coincidences between two protons from pp elastic scattering in the target. Two types of pp elastic scattering events are detected. Type I events, covering an angular range of $\theta_{\text{lab}} = 5 - 35°$, are detected as coincidence between forward scintillators and recoil detectors. The forward scintillators are two plastic scintillators (E and K) and recoil detectors are eight silicon micro strip detectors $(R1-8)$ mounted at azimuthal angles $\pm 45°$ and $\pm 135°$ around the storage cell. Position and angle information for the event is provided by two wire chambers (XY and UV) for the forward scattered proton, and the micro strip position for the recoil.

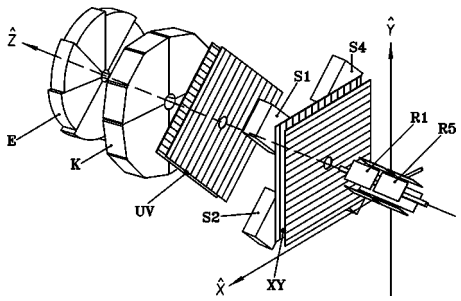

FIG. 2. Schematic view of the detector setup. The forward detector stack consists of two scintillation counters (E,K) and two wire chambers (XY,UV) with two planes each. Recoil protons are detected by eight silicon microstrip detectors surrounding the target cell (R1–8). Large angle detectors (S1–4) detect particles close to $\theta_{\text{lab}} = 45°$.

Type II events, covering the angular range of $\theta_{\text{lab}} = 30° - 60°$ are detected as coincidence between two of four scintillators (S1–4), mounted between the two wire chambers at azimuthal angles $\pm 45°$ and $\pm 135°$. For these events, both protons pass the first wire chamber (XY), allowing reconstruction of angles and origin of the event.

Both event types are subjected to a kinematic fit to determine scattering angle θ, azimuthal angle ϕ, and vertex position z assuming the event originates on the beam axis and follows pp elastic scattering kinematics (see Ref. [1]). To avoid sensitivity to the physical boundaries of roughly $\pm 20°$ around the nominal azimuthal center positions $(\pm 45°, \pm 135°)$ of the recoil (R1-8) and scintillation detectors (S1-S4), only events within $\pm 18.5°$ are accepted. For event type I an additional cut on the correlation between energy loss in the recoil detectors and scattering angle is applied (see Ref. [1]).

For a more detailed description of target, detector system and event selection the reader is referred to Ref. [1]. The measurement was organized in cycles consisting of 3 min injection of polarized beam at 197.4 MeV and 3 min data taking. At the end of a cycle, the beam remaining in the ring was discarded, and the next cycle begins with injection of new beam. Approximately every 30 min, the polarization direction of the injected beam was reversed at the ion source.

The data acquisition was subdivided into 12 s subcycles, in which the target polarization direction was cycled in 2 s intervals through the 6 possible states $(\pm x, \pm y, \pm z)$. The current of the stored beam ranged from 50 to 150 μA with beam lifetimes of 2000–3000 s. A total of approximately 3×10^6 pp elastic scattering events in 12 spin combinations were acquired in 6 days.

IV. DETERMINATION OF THE SPIN CORRELATION PARAMETER A_{zz}

For all orientations of the target holding field (x, y, or z), yields $Y_{ik}(\theta)$ are measured as a function of scattering angle. The experiment uses four different ranges of azimuthal

angles ϕ_i centered at $\phi = \pm 45°$ and $\pm 135°$ and four different combination of beam and target polarization k $(++,+-,-+,--)$. Thus for each orientation of the target guide field, the yields Y_{ik} are represented by a 4×4 matrix. These yields can be related to the pp elastic scattering cross section by factors that contain detector efficiencies on one hand, and luminosities (target thickness, number of incident protons) for the different beam and target polarization combinations on the other hand. Multiplication of the rows i of Y_{ik} by suitable efficiency factors ϵ_i and multiplication of the columns by luminosity factors λ_k yields a matrix $X_{ik} = \epsilon_i Y_{ik} \lambda_k$. Efficiency factors compensate for differences in the detector efficiencies, while luminosity factors normalize the luminosities such that for unpolarized beam and target $X_{ik}^{\mathrm{unpol}} = 1$ for all i,k. The X_{ik} are related to the cross section by $X_{ik} = \sigma_{ik}/\sigma_0$ where σ_0 is the unpolarized differential cross section and σ_{ik} the spin dependent cross section for the specific beam polarization $\vec{P} = (P_x, P_y, P_z)$ and target polarization $\vec{Q} = (Q_x, Q_y, Q_z)$. The method used to determine the X_{ik} from the measured yields Y_{ik} is known as diagonal scaling and described in detail in Ref. [8]. For each scattering angle θ, the experiment yields 48 values of X_{ik} (6 target spin directions, two beam spin directions, four azimuthal angles), which are used to determine experimental quantities of the form (polarization) $\times$ (analyzing power A_y), and (beam polarization) $\times$ (target polarization) $\times$ (spin correlation parameters A_{ik}) (see Ref. [8]). All data are simultaneously analyzed as described in Ref. [1], allowing for possible differences in polarization when the sign of beam and target polarization is reversed, as well as small deviations of the target polarizations from the ideal orientation.

However, for the purpose of illustration, we discuss here the case of longitudinal beam polarization with negligible transverse components $(P_x = P_y = 0)$. For purely longitudinal beam polarization, the X_{ik} are given by

$$X_{ik} = 1 + A_y(Q_x \sin\phi + Q_y \cos\phi) + A_{xz} P_z (Q_y \sin\phi + Q_x \cos\phi) + A_{zz} P_z Q_z . \tag{4.1}$$

Measurements with longitudinal beam polarization P_z and longitudinal target polarization Q_z (with $Q_x = Q_y = 0$) determine the angular distribution $A_{zz}(\theta)$ within a scale factor given by $P_z Q_z$.

Neither P_z nor Q_z can be measured directly since the longitudinal analyzing power A_z vanishes by parity conservation. The method to determine P_z and Q_z used here is based on the assumption (discussed below) that the target polarization Q is independent of orientation of the target spin $(Q = Q_x = Q_y = Q_z)$. Part of this assumption $(Q_x = Q_y)$ has been explicitly verified in Ref. [3]. Since A_{xz} is known from previous measurements, $P_z Q_x$ and $P_z Q_y$ can be determined from the measurements with transverse target polarization, which yield values of $A_{xz}(\theta) P_z Q_x$ and $A_{xz}(\theta) P_z Q_y$. Using the known values of A_{xz}^{in} from Ref. [1] as input, the product $k_{x(y)} = P_z Q_{x(y)}$ of beam and target polarization is varied to minimize the χ^2 between the present results for $P_z Q_x A_{xz}(\theta)$ [or $P_z Q_y A_{xz}(\theta)$] and the scaled A_{xz}^{in}:

$$\chi^2 = \sum_\theta \frac{(P_z Q_{x(y)} A_{xz} - k_{x(y)} A_{xz}^{\mathrm{in}})^2}{[\delta(P_z Q_{x(y)} A_{xz})^2 + (k_{x(y)} \delta A_{xz}^{\mathrm{in}})^2]} . \tag{4.2}$$

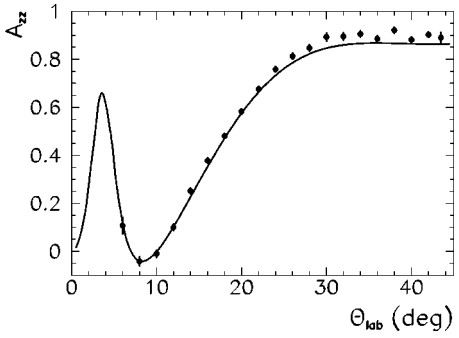

FIG. 3. Angular distribution of the spin correlation parameter A_{zz}. The solid line is the prediction from the partial wave analysis NI93.

Since the analysis uses data over a wide range of angles (5.5° to 43.5°), the final results are of high statistical accuracy. Best agreement with A_{xz}^{in} is obtained for $P_z Q_x = 0.4267 \pm 0.0051$ for target polarization along x and $P_z Q_y = 0.4225 \pm 0.0055$ when the target polarization is along y. The weighted mean $P_z Q = 0.4248 \pm 0.0037$ (or 0.9% relative uncertainty) was used to determine $A_{zz}(\theta)$. The absolute calibration of the resulting $A_{zz}(\theta)$, which ultimately depends on the A_y calibration point [4] which was used in the determination of A_{xz}^{in}, has an overall uncertainty of 2.66%. This uncertainty can be reduced further as will be explained in Sec. V. The final results for A_{zz} are shown in Fig. 3.

The absolute normalization of $A_{zz}(\theta)$ depends on the assumption that PQ with target polarization along z is the same as for target polarization along x or y. The beam polarization P can be assumed independent of the (<1 mT) guide field over the target since the polarization lifetime of the stored beam is very long (>1 h [9]) compared to the rapid (6 s) sequence of target polarization states. In an earlier experiment with transverse beam polarization, independence of P on guide field direction was confirmed by direct measurement to better than 0.5% (see Table 1 in Ref. [1]).

We now discuss the assumption that the magnitude of the target polarization does not depend on orientation. Change in the target polarization direction is accomplished by changing the guide field in the target region, which is provided by three sets of coils external to the vacuum system [3]. Information on the uniformity and accuracy of the guide field direction over the target, and effects of the guide field on the proton closed orbit is given in Ref. [3]. The absolute value of the polarization of the gas target is independent of the orientation and sign of the guide field because between the exit of the last sixpole magnet of the atomic beam source and the target cell the spin of the atoms follow the magnetic field direction adiabatically: from an initially inhomogeneous field in the sixpole, as the atoms travel into the homogeneous field

at the target, the magnetic moments follow the field direction, no matter what the orientation of the guide field is.

The condition of adiabaticity requires that along the trajectory of the atoms the field direction changes experienced by the atoms are slow compared to the Larmor precession rate of the atom in that field. That this condition is easily met is evident from the many polarized ion sources based on the atomic beam method, that provide large polarization without making special provisions to assure adiabaticity. However, if there is a point between atomic beam source and target, where the magnetic field is both small in magnitude (low Larmor frequency) and changing rapidly in field direction, loss of polarization arises. This loss may depend on the direction of the guide field over the target, because fringe fields of the guide field coils may under some conditions nearly cancel the ambient field. Consequently, careful field measurements were made along the atomic beam axis for each of the six different target guide field conditions. The rate of change in the field direction compared to the Larmor precession rate was found to be less than 5×10^{-6} and satisfies the adiabaticity condition of being $\ll 1$.

The second concern is the possibility that the transition unit [medium-field transition (MFT)], which is used in the atomic beam source to select a single hyperfine state of hydrogen atoms, may be affected by the fringe field of the guide field coils. While it is found that the resonance region shifts slightly when the x guide field is reversed, the resonance region is wide enough (see Ref. [10]) that a working point exists for which the transition works properly for all guide field orientations.

Finally, the expectation that the product of beam and target polarization is independent of guide field can be checked directly for guide fields along x and y. No statistically significant difference has been observed, neither in this experiment, nor in previous experiments with transverse beam polarization [1,3].

V. ABSOLUTE NORMALIZATION

The absolute normalization of the present A_{zz} data and the previously reported values of A_{xx}, A_{yy}, and A_{xz} [1,3] all depend on the A_y calibration point reported in Ref. [4]. The calibration can be checked and the accuracy of the calibration can be improved by use of the identity

$$A_{yy}-A_{xx}-A_{zz}\equiv 1, \tag{5.1}$$

which applies to spin correlation coefficients in elastic scattering of spin 1/2 particles at a center of mass angle of 90°. The relation follows directly from symmetry relations between the five helicity amplitudes at that scattering angle [5].

To improve the statistical accuracy of the experimental value of $S=A_{yy}-A_{xx}-A_{zz}$ at $\theta_{\rm c.m.}=90°$ ($\theta_{\rm lab}=43.57°$), a polynomial fit of the angular distribution of $A_{yy}-A_{xx}-A_{zz}$ was performed in the vicinity of $\theta_{\rm lab}=43.57°$. Because the spin correlation coefficients are symmetric around $\theta_{\rm c.m.}=90°$, the angular distribution has an extremum at the corresponding laboratory angle of $\theta_{\rm lab}=43.57°$ so that only even terms with extrema at this laboratory angle were used as fitting functions.

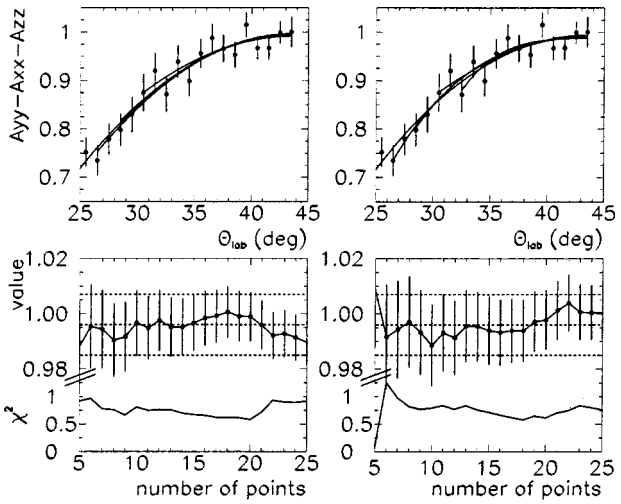

FIG. 4. Examples of parabolic and fourth order fits to the angular distribution of $A_{yy}-A_{xx}-A_{zz}$ used in the determination of the value at $\theta_{\rm c.m.}=90°$ ($\theta_{\rm lab}=43.57$). The top two panels show the data points and polynomial fits (parabolic: left, fourth order: right), the bottom panels show the corresponding value of $A_{yy}-A_{xx}-A_{zz}$ at $\theta_{\rm c.m.}=90°$ (left scale, points) and χ^2 of the fits (right scale, solid line). The dashed lines indicate the selected value and its uncertainty.

Figure 4 shows examples for parabolic fits and fits including a second and fourth order term. The extracted values of S are insensitive to the number of data points used as long as the $\chi^2/$ (degree of freedom) of the fits is close to its mimimum (see bottom panels in Fig. 4). For 10–20 data points included in the fits, the extracted values vary by ± 0.005, which is taken into account as an interpolation uncertainty.

To test the accuracy of the above procedure, simulated data were produced from predictions for the A_{ik} from partial wave analyses for the laboratory angular range 23° to 43.5° (corresponding to 20 data points). The values for S differed from the correct value $S\equiv 1$ by less than 10^{-3}.

The result for the sum S is taken from the parabolic fit with 14 data points

$$S=(A_{yy}^{90}-A_{xx}^{90}-A_{zz}^{90})=0.996\pm 0.011, \tag{5.2}$$

where the uncertainty contains statistical and interpolation uncertainties added in quadrature. The final values for the angular distribution of A_{zz} were determined by dividing the A_{zz} obtained in Sec. IV, which were normalized to the A_{xz} from [1] by $S=0.996$ in order to satisfy the identity Eq. (5.1). The results are given in Table I.

The absolute normalization uncertainty of the spin correlation coefficients is affected by two factors: the 1.1% error in S and the relative uncertainty in the determination of P_zQ which is given as 0.9% in Sec. IV. The error analysis must take into account that changing P_zQ by 0.9% requires a change in A_{zz} and a change in $A_{yy}-A_{xx}$ if the identity Eq. (5.1) is to be maintained. Numerical calculations show that

TABLE I. Final results for the angular distribution of the spin correlation parameter A_{zz}, using the relation $A_{yy}-A_{xx}-A_{zz}\equiv 1$ for the normalization. The absolute normalization uncertainty is 2.0%.

$\theta_{\rm lab}$ (deg)	A_{zz}	δA_{zz}	$\theta_{\rm lab}$ (deg)	A_{zz}	δA_{zz}
5.5	0.267	0.078	25.5	0.793	0.021
6.5	0.063	0.041	26.5	0.835	0.022
7.5	−0.056	0.033	27.5	0.854	0.023
8.5	−0.032	0.027	28.5	0.840	0.024
9.5	−0.037	0.024	29.5	0.897	0.026
10.5	0.014	0.023	30.5	0.888	0.028
11.5	0.067	0.022	31.5	0.855	0.027
12.5	0.130	0.021	32.5	0.932	0.026
13.5	0.200	0.020	33.5	0.887	0.024
14.5	0.298	0.019	34.5	0.923	0.023
15.5	0.341	0.019	35.5	0.887	0.023
16.5	0.412	0.018	36.5	0.883	0.022
17.5	0.464	0.018	37.5	0.913	0.021
18.5	0.497	0.018	38.5	0.928	0.020
19.5	0.554	0.018	39.5	0.855	0.020
20.5	0.612	0.018	40.5	0.906	0.019
21.5	0.663	0.019	41.5	0.924	0.019
22.5	0.689	0.019	42.5	0.883	0.018
23.5	0.734	0.020	43.5	0.890	0.024
24.5	0.786	0.021			

an increase of P_zQ by 0.9% reduces A_{zz} by 1.6% and increases $A_{yy}-A_{xx}$ by 0.8%. Adding the statistical error of S in quadrature yields a final scale uncertainty of 2.0% for the A_{zz} in Table I.

The present results suggest that the values of the A_{ik} reported in Ref. [1] should be divided by $S=0.996$ and should be assigned a scale uncertainty of 1.4%. Since the measurement of A_y in Ref. [1] only involves either a beam or a target polarization, the values should be divided by $\sqrt{S}=0.998$ and assigned a 0.7% uncertainty.

VI. CORRECTIONS

In this section a summary of small corrections applied to the final results will be given. As the methods used to determine these corrections are discussed elsewhere [1], only a brief overview is given here.

A. Deadtime

Deadtime of the data acquisition system is of concern because the total event rate changes by some 40% between parallel and antiparallel beam and target helicities. The fractional dead time was determined by using fast scalers to count the number of events presented to the data acquisition computer compared to the number of processed events. These scalers were read once a second. The loss rate is found to be a linear function of the rate of accepted events (Fig. 5). From the slope a deadtime per processed event of 232 ± 7 μs is found. The average loss probability is about 3 and 5% for parallel and antiparallel beam and target spins, respectively. Before executing the polarization analysis, the yields are corrected for the number of lost events. The deadtime correction increases the value of A_{zz} by about 0.014, or 2/3 of the statistical error. This is by far the largest correction that needed to be applied.

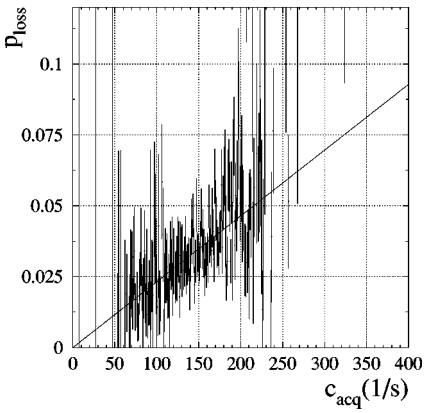

FIG. 5. Typical plot of the probability $p_{\rm loss}$ of losing an event because of deadtime versus the rate of accepted (processed) events $c_{\rm acq}$. The solid line is a linear fit. The slope determines the deadtime per event τ.

B. Finite θ-bin correction

The angular distribution of the spin correlation coefficient A_{zz} is reported at the center of 1° $\theta_{\rm lab}$ angle bins and the entire analysis was executed with this binning. Since both cross section and polarization observables depend on angle, the values at the center of the bin may differ slightly from the measured mean over the bin.

The measured angular distributions of the spin correlation parameters A_{xz} used for normalization and A_{zz} are corrected for this effect. The correction to A_{zz} is typically 0.001. For angles below 10°, where the acceptance of the detector system is angle dependent, the correction changes to about 0.006 and becomes comparable with the statistical error for the two smallest angle bins. The effect on the normalization was found to be less than 0.07% and is neglected, as the overall norm error is 2.0%.

C. Correction for nonuniform ϕ acceptance

In the polarization analysis we assume that the acceptance of the detector system as a function of the azimuthal angle ϕ is uniform. However, the data show that the ϕ acceptance depends slightly on the scattering angle $\theta_{\rm lab}$ and is in general not uniform.

The term containing the spin correlation parameter A_{zz} has no ϕ dependence, thus there is no effect on the angular distribution of A_{zz}. However, the ϕ dependence of the A_{xz} term, required a correction of -0.001 to the absolute normalization of A_{zz}. This correction is well below the absolute error of the norm and the treatment as a small correction is justified.

D. Background

Although the storage cell wall is made of thin Teflon foils, it is still about 10^9 times more massive than the polar-

TABLE II. Table with χ^2 per datapoint for the comparison of the data to potential models and partial wave analyses. The second column contains the χ^2 between the present A_{zz} results and the predictions. Columns three and four contain the χ^2 and scaling factor k_s by which the A_{zz} data need to be multiplied to yield the best agreement between prediction and data. Column five gives the overall χ^2 per degree of freedom for A_y and all spin correlation parameters (A_{xx}, A_{yy}, A_{xz}, A_{zz}). The A_y and A_{ik} are multiplied by factors k_s' and $k_s'^2$, respectively, adjusted for best agreement with each calculation. The data for A_y and A_{xx}, A_{yy}, A_{xz} are from Ref. [1], to which the small correction described in Sec. V was applied.

	A_{zz}	A_{zz} scaled		A_y and all A_{ik} scaled	
Prediction	χ^2	χ_s^2	k_s	$\chi_s'^2$	k_s'
AV18	4.03	1.50	0.975	1.65	0.988
REID93	2.09	0.70	0.981	1.24	0.991
CDBonn	3.27	1.32	0.978	1.44	0.989
Paris80	4.56	1.01	0.970	4.27	0.986
Ni93	2.00	0.72	0.978	1.31	0.991
NI97	2.24	0.77	0.980	1.12	0.989
SM94	5.29	4.41	0.985	5.41	0.997
WI96	5.76	3.36	0.976	3.39	0.996
SM97	2.34	0.92	0.981	1.97	0.990
SP99	1.92	0.79	0.983	1.51	0.990

ized hydrogen gas stored inside, so that interaction of the beam halo with the cell wall presents a potential source of background. In previous experiments with the present setup, different methods for investigation of possible background events were explored. It was found that the tightest limit on background events entering the final p-p elastic data is obtained if the polarized hydrogen data is compared with data taken when N_2 is admitted to the target. Background events, such as reactions on the C and F nuclei in the Teflon cell walls as well as with N_2, are in general lacking the coplanarity of pp elastic scattering. Noncoplanar events recorded with the polarized hydrogen target can be used to estimate the number of coplanar events not originating from the target gas that enter the final yields. For details see Ref. [1].

The limit on the fractional background in the final data is found to be $<0.5\%$. As the normalization is based on measurements with x and y orientation of the holding field, and the angular distribution for A_{zz} is determined from the measurement with the z orientation, only a dependence of the background on the holding field orientation would affect the results. Within the 0.1% statistical uncertainty in the determination of the fractional background no dependence on the holding field direction was found.

The effect of the background on the final results for A_{zz} was estimated from a simulation of yields with and without added background, and the effect was found to be less than 10% of the statistical errors. No correction to the results was applied.

VII. COMPARISON TO THEORY

In Ref. [1], angular distributions of the analyzing power A_y and three spin correlation coefficients (A_{xx}, A_{yy}, A_{xz}) were compared to current partial wave analyses (PWA) (Nijmegen group: Ni93 [11], Ni97 [12]; Virginia group: SM94, SM97 [13]) and to a number of potential model calculations (Reid93 [14,12], Argonne potential AV18 [15,16], CD-Bonn [17,13], Paris80 [18,13]). In Table II, the columns labeled χ^2 shows the quality of agreement for some of these calculations, as well as for the most recent VPI analysis SP99 [13], which already includes the current results for A_{zz}. Best agreement (χ^2 per point ≈ 2) is found for the Nijmegen PWA analyses (Ni93, Ni97) which is based on a fit to NN data in the energy range 0–350 MeV, and the most recent VPI analyses (SM97, SP99), which analyzed data up to 2500 MeV. Similar quality of agreement is observed for the updated Reid potential (Reid93) constructed by the Nijmegen group.

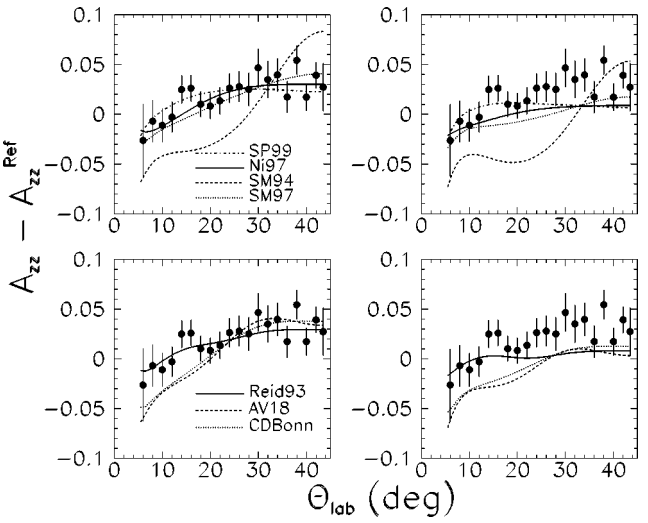

FIG. 6. Comparison between A_{zz} and partial wave analyses (top) and predictions from potential models (bottom). The data and predictions are plotted as difference to the reference NI93. The left two panels show predictions divided by the scaling factors giving best agreement with the predictions and the A_{zz} data (column 4 of Table II). The right two panels use the factors k_s' from scaling A_y and all A_{ik} (column 6 of Table II).

The agreement between A_{zz} and various calculations is improved if one allows the normalization to float. If beam and target polarization calibration are each reduced by a factor k, the spin correlation coefficients multiply by k^2. The columns labeled ''A_{zz} scaled'' (Table II) show significant improvement when the measured $A_{zz}(\theta)$ are reduced [or the calculated $A_{zz}(\theta)$ are increased] by about 3% ($k_s=0.985$, or $k_s^2=0.970$), in which case the best calculations yield a χ_s^2 per degree of freedom near 1. The values for the scaling factors k_s are not incompatible with the uncertainty of 2.0% of the absolute normalization.

Comparison between data and (scaled) calculations is shown on the left hand side of Fig. 6. For presentation in the figures, the data are rebinned in 2° bins by taking the weighted mean of neighboring 1° bins. As was done in Ref. [1], reference value $A_{zz}^{\rm ref}$ (calculated from the Ni93 PWA) were subtracted from the measured A_{zz} and all calculations in order to display small differences more clearly. For convenience, we plot the (unscaled) A_{zz} data points and instead

scale the calculations by the appropriate factors, since the scaled data points would be different for each calculation. The figure shows that the most recent phase shift analyses, as well as the Nijmegen version of the Reid potential, are in excellent agreement with the measurements, when the scale factors listed in Table II are applied.

The analysis was repeated to include the previous data [1] on A_y and A_{ik} at the same energy. In accordance with Sec. V, the published values of A_y and A_{ik} were divided by 0.998 and 0.996, respectively. The last two columns of Table II give the overall χ^2 per degree of freedom ($\chi_s'^2$) if the measured A_y and all A_{ik} are multiplied by factors k_s' and $k_s'^2$, respectively. Good overall agreement is found for the Reid93 potential ($\chi_s'^2=1.24$) and for the most recent phase shift analyses Ni97 ($\chi_s'^2=1.12$) and SP99 ($\chi_s'^2=1.51$), where the new SP99 analysis by the GW/VPI group already took advantage of the present A_{zz} data. For SP99 in particular, the agreement with the present A_{zz} data is excellent. The agreement of these calculations with the A_{zz} reported here is shown on the right hand side of Fig. 6. According to Table II, the scale correction for the A_{ik} is around 2% for Reid93 and Ni97 and SP99, which is compatible with the experimental scale uncertainty for the A_{ik} of [1] of 1.4% and the A_{zz} of 2% (Sec. V).

It should be mentioned that the above comparisons have the defect that the same scale factor was applied to A_{zz} and to the A_{ik} of [1], while indeed it was pointed out in Sec. V that the component of the scale uncertainty that arises from the A_{xz} comparison is different for A_{zz} and the other A_{ik}.

VIII. CONCLUSIONS

A beam of polarized protons whose polarization in the target region is along the beam direction was developed at the IUCF Cooler synchrotron. Since the spin precesses in the bending magnets, stable longitudinal polarization in the target straight section required the introduction of solenoids. Limitations of the available solenoid strength caused a deviation from the ideal longitudinal polarization, but the remaining transverse beam polarization components are small and easily taken into account in the data analysis. We believe this is the first time that stable longitudinal beam polarization has been used for a nuclear physics measurement in a proton storage ring.

The 197.4 MeV beam was incident on a polarized H gas target, whose polarization was changed in 2 s intervals between six different orientations ($\pm x, \pm y, \pm z$) by changing a weak guide field over the target. Longitudinal target polarization allowed the determination of the spin correlation parameter A_{zz}. Elastically scattered protons were detected in coincidence in silicon-strip recoil detectors and in scintillators and wire chambers in forward direction. The effect of background events was investigated and found negligible. The only significant correction was for deadtime losses, which are spin dependent because of count rate changes between parallel and antiparallel beam and target spins.

Measurements of A_{zz} were obtained for laboratory angles between 5.5° and 43.5° ($\theta_{\text{c.m.}}=11.5°-90°$) in 1° intervals with a statistical error of about 0.02. Except for a limited amount of data at 305 MeV [19] in a narrow angular range near $\theta_{\text{c.m.}}=90°$ this is the only A_{zz} data in pp scattering below the pion threshold.

The identity $A_{yy}-A_{xx}-A_{zz}\equiv 1$ at $\theta_{\text{c.m.}}=90°$ is exploited to check the absolute calibration of earlier spin correlation measurements by our group [1] and to provide an improved absolute calibration of the data. In order to relate the product PQ of beam and target polarization in the present experiment to the PQ calibration in the determination of A_{xx} and A_{yy} in Ref. [1], measurements here were taken at the same time with transverse target polarization. This allowed relating the calibration in the two experiments via the common measurement of the spin correlation parameter A_{xz}. The result determined the absolute calibration of the present A_{zz} angular distribution to an accuracy of $\pm 2.0\%$. The above identity also allows a recalibration of the absolute normalization for the results of Ref. [1]. The new calibration would multiply the A_y by 1.002 and the A_{ik} by 1.004, which is well within the uncertainties reported in Ref. [1].

In addition to the inherent interest in measuring A_{zz} to complete the entire set of independent spin correlation parameters in pp elastic scattering at 197.4 MeV, the measurements have particular significance since they strengthen the absolute polarization calibration over the entire energy range from 200 to 450 MeV [20], which was based on exporting the 200 MeV calibration to the higher energies.

ACKNOWLEDGMENTS

We are grateful for the efforts of the accelerator operation group at IUCF, in particular D. Friesel and T. Sloan. This work was supported in part by the National Science Foundation and the Department of Energy. One of us (F.R.) would also like to thank the Alexander von Humboldt Foundation for their generous support.

[1] F. Rathmann, B. von Przewoski, W. A. Dezarn, J. Doskow, M. Dzemidzic, W. Haeberli, J. G. Hardie, B. Lorentz, H. O. Meyer, P. V. Pancella, R. E. Pollock, T. Rinckel, F. Sperisen, and T. Wise, Phys. Rev. C **58**, 658 (1998).

[2] B. von Przewoski, F. Rathmann, W. A. Dezarn, J. Doskow, M. Dzemidzic, W. Haeberli, J. G. Hardie, B. Lorentz, H. O. Meyer, P. V. Pancella, R. E. Pollock, T. Rinckel, F. Sperisen, and T. Wise, Phys. Rev. C **58**, 1897 (1998).

[3] W. Haeberli, B. Lorentz, F. Rathmann, M. A. Ross, T. Wise, W. A. Dezarn, J. Doskow, J. G. Hardie, H. O. Meyer, R. E. Pollock, B. von Przewoski, T. Rinckel, F. Sperisen, and P. V. Pancella, Phys. Rev. C **55**, 597 (1997).

[4] B. von Przewoski, H. O. Meyer, P. V. Pancella, S. F. Pate, R. E. Pollock, T. Rinckel, F. Sperisen, J. Sowinski, W. Haeberli, W. K. Pitts, and J. S. Price, Phys. Rev. C **44**, 44 (1991).

[5] J. Bystricky, F. Lehar, and P. Winternitz, J. Phys. (France) **39**,

1 (1978); G. G. Ohlsen, Rep. Prog. Phys. **35**, 717 (1972).
[6] V. Bargmann, L. Michel, and V. L. Telegdi, Phys. Rev. Lett. **2**, 435 (1959).
[7] B. W. Montague, Phys. Rep. **113**, 1 (1984).
[8] H. O. Meyer, Phys. Rev. C **56**, 2074 (1997).
[9] H. O. Meyer, B. Lorentz, M. Dzemidzic, J. Doskow, W. Haeberli, P. V. Pancella, R. E. Pollock, B. v. Przewoski, F. Rathmann, T. Rinckel, F. Sperisen, and T. Wise, Phys. Rev. E **56**, 3578 (1997).
[10] A. Roberts, P. Elmer, M. A. Ross, T. Wise, and W. Haeberli, Nucl. Instrum. Methods Phys. Res. A **322**, 6 (1992).
[11] V. J. G. Stoks, R. A. M. Klomp, M. C. M. Rentmeester, and J. J. DeSwart, Phys. Rev. C **48**, 792 (1993).
[12] J. J. DeSwart and M. C. M. Rentmeester (private communication).
[13] The SAID dial-in. Available via TELNET to said.phys.vt.edu, with userid:said (no password required).
[14] V. G. J. Stoks, R. A. M. Klomp, C. P. F. Terheggen, and J. J. de Swart, Phys. Rev. C **49**, 2950 (1994).
[15] V. G. J. Stoks (private communication).
[16] R. B. Wiringa, V. G. J. Stoks, and R. Schiavilla, Phys. Rev. C **51**, 38 (1995).
[17] R. Machleidt, Phys. Rev. C **53**, 1483 (1996).
[18] M. Lacombe *et al.*, Phys. Rev. C **21**, 861 (1980).
[19] I. P. Auer *et al.*, Phys. Rev. D **29**, 2435 (1984).
[20] R. E. Pollock, W. A. Dezarn, M. Dzemidzic, J. Doskow, J. G. Hardie, H. O. Meyer, B. v. Przewoski, T. Rinckel, F. Sperisen, W. Haeberli, B. Lorentz, F. Rathmann, T. Wise, and P. V. Pancella, Phys. Rev. E **55**, 7606 (1997).